Brivanib Alaninate, a Dual Inhibitor of Vascular Endothelial Growth Factor Receptor and Fibroblast Growth Factor Receptor Tyrosine Kinases, Induces Growth Inhibition in Mouse Models of Human Hepatocellular Carcinoma

Hung Huynh,[1] Van Chanh Ngo,[1] Joseph Fargnoli,[4] Mark Ayers,[5] Khee Chee Soo,[2] Heng Nung Koong,[2] Choon Hua Thng,[1] Hock Soo Ong,[2] Alexander Chung,[2] Pierce Chow,[3] Pamela Pollock,[6] Sara Byron,[6] and Evelyn Tran[1]

Abstract

Purpose: Hepatocellular carcinoma (HCC) is the fifth most common primary neoplasm; surgery is the only curative option but 5-year survival rates are only 25% to 50%. Vascular endothelial growth factor (VEGF) and fibroblast growth factor (FGF) are known to be involved in growth and neovascularization of HCC. Therefore, agents that target these pathways may be effective in the treatment of HCC. The aim of this study was to determine the antineoplastic activity of brivanib alaninate, a dual inhibitor of VEGF receptor (VEGFR) and FGF receptor (FGFR) signaling pathways.

Experimental Design: Six different s.c. patient-derived HCC xenografts were implanted into mice. Tumor growth was evaluated in mice treated with brivanib compared with control. The effects of brivanib on apoptosis and cell proliferation were evaluated by immunohistochemistry. The SK-HEP1 and HepG2 cells were used to investigate the effects of brivanib on the VEGFR-2 and FGFR-1 signaling pathways *in vitro*. Western blotting was used to determine changes in proteins in these xenografts and cell lines.

Results: Brivanib significantly suppressed tumor growth in five of six xenograft lines. Furthermore, brivanib–induced growth inhibition was associated with a decrease in phosphorylated VEGFR-2 at $Tyr^{1054/1059}$, increased apoptosis, reduced microvessel density, inhibition of cell proliferation, and down-regulation of cell cycle regulators. The levels of FGFR-1 and FGFR-2 expression in these xenograft lines were positively correlated with its sensitivity to brivanib-induced growth inhibition. In VEGF-stimulated and basic FGF stimulated SK-HEP1 cells, brivanib significantly inhibited VEGFR-2, FGFR-1, extracellular signal-regulated kinase 1/2, and Akt phosphorylation.

Conclusion: This study provides a strong rationale for clinical investigation of brivanib in patients with HCC.

Hepatocellular carcinoma (HCC) is the fifth most common primary neoplasm, accounting for approximately 667,000 deaths worldwide annually (1, 2). Recurrence, metastasis, or the development of new primary tumors is the most common cause of mortality for patients with HCC (3, 4). Surgery is the only proven potentially curative therapy for HCC; however, only 10% to 20% of patients undergo surgery because of poor liver function, metastases, or both (5–7), and of those having surgery, the 5-year survival rate is only 25% to 50%. Several chemotherapeutic agents have been evaluated for the treatment of HCC; however, no single or combination chemotherapy regimen is particularly effective (8). Doxorubicin is the most widely used agent in HCC; studies have shown a 4% to 10.5% response rate in patients with HCC (9, 10). However, the overall response rate, but not overall survival, was shown to double when doxorubicin was given in combination with cisplatin, IFN, and 5-fluorouracil (10). The multitargeted tyrosine kinase inhibitor sorafenib (Nexavar, Bayer and Onyx Pharmaceuticals), which inhibits vascular endothelial growth factor receptor (VEGFR), platelet-derived growth factor receptor, raf, c-kit, and flt-3, has been shown to inhibit HCC-induced proliferation and angiogenesis (11). More recently, sorafenib has been shown to provide a significant improvement in overall

Authors' Affiliations: [1]Laboratory of Molecular Endocrinology, Division of Cellular and Molecular Research, National Cancer Centre; Departments of [2]General Surgery and [3]Experimental Surgery, Singapore General Hospital, Singapore, Singapore; [4]Discovery Biology and [5]Discovery Medicine and Clinical Pharmacology, Bristol-Myers Squibb, Princeton, New Jersey; and [6]Cancer and Cell Biology Division, Translational Genomics Research Institute, Phoenix, Arizona

Received 2/25/08; revised 4/24/08; accepted 5/7/08.

Grant support: Singapore Cancer Syndicate grants SCS-AS0032, SCS-HS0021, and SCS-AMS0086 (H. Huynh).

The costs of publication of this article were defrayed in part by the payment of page charges. This article must therefore be hereby marked *advertisement* in accordance with 18 U.S.C. Section 1734 solely to indicate this fact.

Requests for reprints: Hung Huynh, Laboratory of Molecular Endocrinology, Division of Cellular and Molecular Research, National Cancer Centre of Singapore, Singapore 169610, Singapore. Phone: 65-436-8347; Fax: 65-226-5694; E-mail: cmrhth@nccs.com.sg.

doi:10.1158/1078-0432.CCR-08-0509

survival in patients with HCC (12), suggesting that this class of agents may be effective in the treatment of HCC.

Brivanib is hydrolyzed to the active moiety BMS-540215 *in vivo*. BMS-540215 shows potent and selective inhibition of VEGFR and fibroblast growth factor receptor (FGFR) tyrosine kinases (13). The structures of brivanib and BMS-540215 are shown in Fig. 1. BMS-540215 is an ATP-competitive inhibitor of human VEGFR-2, with an IC_{50} of 25 nmol/L and K_i of 26 nmol/L. In addition, it inhibits VEGFR-1 (IC_{50} = 380 nmol/L) and VEGFR-3 (IC_{50} = 10 nmol/L). BMS-540215 also showed good selectivity for FGFR-1 (IC_{50} = 148 nmol/L), FGFR-2 (IC_{50} = 125 nmol/L), and FGFR-3 (IC_{50} = 68 nmol/L). Furthermore, BMS-540215 has been shown to selectively inhibit the proliferation of endothelial cells stimulated by VEGF and FGF *in vitro* with IC_{50} values of 40 and 276 nmol/L, respectively (13). It also shows broad-spectrum *in vivo* antitumor activity over multiple dose levels and induces stasis in large tumors, suggesting that it may have a role in the treatment of HCC.

High expression of angiogenic factors VEGF, basic FGF (bFGF), and insulin-like growth factor (IGF)-2 is detected in 2 patients with HCC (14–17), and when released from tumor cells, inflammatory cells, and/or tumor stromal cells, they participate in the neovascularization and metastatic potential of HCC (18–20). VEGF is considered one of the most important of all of the angiogenic factors involved in HCC vascularization. Plasma VEGF levels are significantly elevated in patients with HCC and distant metastasis (21), and the increased expression of VEGF is correlated with histologic tumor grade (22) and tumor microvessel density (23). In addition, high preoperative serum levels of VEGF are predictive of microscopic venous invasion (24) and poor response to chemoembolization (25). bFGF or FGF-2 is also a potent angiogenic factor in HCC (14, 26, 27). bFGF stimulates the release and activity of collagenases, proteases, and integrins on the extracellular membrane to form nascent microvascular networks (28). The expression of heparanase in connection with bFGF enhances growth, invasion, and angiogenesis of the tumor (29). Indeed, in a clinical study of patients undergoing resection of HCC, a high preoperative serum bFGF level seemed to be predictive of invasive tumor and early postoperative recurrence (30). Furthermore, bFGF has been shown to synergistically augment VEGF-mediated HCC development and angiogenesis (31). It functions as a mitogen for HCC cell proliferation via an autocrine mechanism and enhances the development and progression of HCC by binding to FGFR-1 (32). Because VEGFRs and FGFRs are both present on endothelial cells and provide critical signaling pathways for HCC metastasis, the use of brivanib that inhibits both VEGFR and FGFR could be of therapeutic importance.

Here, we report the results of a study assessing the effects of brivanib, a dual VEGFR and FGFR inhibitor, on tumor growth and apoptosis in mouse models of human HCC, which have previously been established and characterized to investigate novel compounds for the treatment of HCC (33).

Materials and Methods

Reagents. Research-grade Capsitol was purchased from CyDex, Inc. Primary antibodies against CD31/platelet endothelial cell adhesion molecule 1, p130 RB, $p21^{WAF1}$, $p27^{Kip1}$, and Ki-67 were from Lab Vision. Anti-Akt (Ser^{473}), anti–extracellular signal-regulated kinase 1/2 (ERK1/2; Thr^{202}/Tyr^{204}), anti–cleaved caspase-3, anti–cleaved poly(ADP-ribose) polymerase (PARP), anti–VEGFR-2, and anti–phospho-VEGFR-2 ($Tyr^{1054/1059}$) were obtained from Cell Signaling Technology. Anti–phospho-c-Myc (Tyr^{58}/Ser^{62}) antibodies were from Epitomics, Inc. Antibodies against FGFR-1, FGFR-2, FGFR-3, FGFR-4, pRB, cyclin D1, cyclin-dependent kinase (Cdk)-2, Cdk-4, cdc-2, cyclin A, cyclin B1, Bax, Bad, Bcl-2, Bcl-x, and α-tubulin were from Santa Cruz Biotechnology, Inc. Recombinant VEGF, platelet-derived growth factor-AB, and IGF-I were purchased from Millipore Corp. Conjugated secondary antibodies were supplied by Pierce. The chemiluminescent detection system was supplied by Amersham Pharmacia Biotech. Tris-base, NaCl, EDTA, EGTA, Triton X-100, sodium pyrophosphate, β-glycerolphosphate, Na_3VO_4, leupeptin, and phenylmethylsulfonyl fluoride were obtained from Sigma Chemical Co.

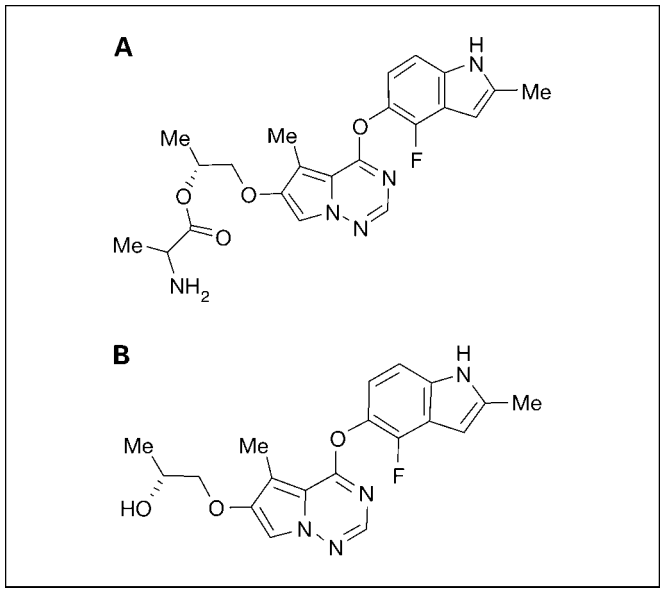

Fig. 1. Structure of brivanib (*A*) and BMS-540215 (*B*).

Cell culture. SK-HEP1 and HepG2 cells were obtained from the American Type Culture Collection. They were maintained in modified Eagle's medium (Life Technologies) supplemented with 10% fetal bovine serum (growth medium). SK-HEP1 cells were selected for *in vitro* studies because they are of endothelial origin cells that express both VEGFR-2 and FGFR-1 (34). To study the effects of brivanib treatment on VEGF- and bFGF-stimulated activation of Akt and ERK1/2 pathways, SK-HEP1 and HepG2 cells were treated with 2 μmol/L brivanib for 24 h and then stimulated with 40 ng/mL VEGF or bFGF. In addition, brivanib SK-HEP1 cells were also stimulated with IGF-1 for 15 min. The cells were lysed and the lysates were analyzed for levels of the effector proteins, including the serine/threonine kinase Akt and ERK1/2.

Xenograft models. This study received ethics board approval at the National Cancer Centre of Singapore and Singapore General Hospital. All mice were maintained according to the Guide for the Care and Use of Laboratory Animals published by the NIH. They were provided with sterilized food and water *ad libitum* and housed in negative pressure isolators with 12-h light/dark cycles.

Previously established patient-derived HCC xenografts (2-1318, 5-1318, 2006, 30-1004, 26-1004, and 06-0606; ref. 33) were s.c. implanted in male severe combined immunodeficient mice ages 9 to 10 wk (Animal Resources Centre). The 2-1318, 5-1318, 06-0606, and 30-1004 xenografts were derived from hepatitis B virus–positive HCC, whereas the 26-1004 xenograft line had wild-type p53. Two xenograft lines (2-1318 and 5-1318) exhibited a mutation in codon 249 of the

p53 gene. A mutation in codon 177 and a frameshift mutation in codon 270 of the *p53* gene were detected in xenograft lines 2006 and 30-1004, respectively. A mutational analysis revealed that xenograft line 26-1004 exhibited a 16-bp deletion in exon 8 of the *PTEN* gene.

Tumor treatment. Brivanib (Bristol-Myers Squibb, Pharmaceutical Research Institute) was diluted in vehicle (30% Capsitol in water) at an appropriate concentration. To investigate the effects of brivanib on the growth of patient-derived HCC xenografts, mice bearing the tumors described above were orally given 50 or 100 mg/kg brivanib daily or 200 μL vehicle for 12 d. For the dose-response experiments, mice bearing the xenograft line 06-0606 were given two doses of brivanib (50 and 100 mg/kg daily) orally starting on day 7 after tumor implantation. Each treatment group comprised 14 animals and each experiment was repeated at least thrice. Treatment started on day 7 after tumor implantation, by which time the patient-derived HCC xenografts were ~100 mm^3 in size. Tumor growth was monitored at least twice weekly by vernier caliper measurement of the length and width of tumor. The tumor volume was calculated as follows: length × $width^2 \times \pi/6$. At the end of the study, the mice were sacrificed with body and tumor weights being recorded, and the tumors were harvested for analysis.

The efficacy of brivanib in reducing tumor growth was analyzed by the treatment to control (T/C) ratio, where T and C are the median weight (mg) of brivanib-treated and vehicle-treated tumors, respectively, on treatment day 12. T/C ratios ≤0.42 are considered an active response according to the Drug Evaluation Branch of the Division of Cancer Treatment, National Cancer Institute criteria.

Western blot analysis. To determine changes in proteins [cleaved caspase-3, cleaved PARP, anti–VEGFR-2, anti–phospho-VEGFR-2 ($Tyr^{1054/1059}$), phospho-c-Myc (Tyr^{58}/Ser^{62}), FGFR-1, FGFR-2, FGFR-3, FGFR-4, pRB, cyclin D1, Cdk-2, Cdk-4, cdc-2, cyclin A, cyclin B1, Bax, Bad, Bcl-2, Bcl-x, and α-tubulin], independent tumors from mice treated with vehicle ($n = 3$) and brivanib ($n = 3$-4) were homogenized in buffer containing 20 mmol Tris (pH 7.5), 150 mmol NaCl, 1 mmol/L EDTA, 1 mmol EGTA, 1% Triton X-100, 2.5 mmol sodium pyrophosphate, 1 mmol β-glycerolphosphate, 2 mmol Na_3VO_4, 1 μg/mL leupeptin, and 1 mmol phenylmethylsulfonyl fluoride (33). The protein concentration was determined by Bio-Rad protein assay (Bio-Rad Laboratories). Western blot analysis of samples (100 μg protein per sample) to analyze the effect of brivanib treatment on markers of apoptosis and cell cycle regulation was undertaken according to standard protocols (35). Blots were incubated with indicated primary antibodies and 1:7,500 horseradish peroxidase–conjugated secondary antibodies. All primary antibodies were used at a final concentration of 1 μg/mL. The blots were then visualized with a chemiluminescent detection system.

Immunohistochemistry. Tumor tissue samples were processed for paraffin embedding and 5-μm sections were prepared. After blocking

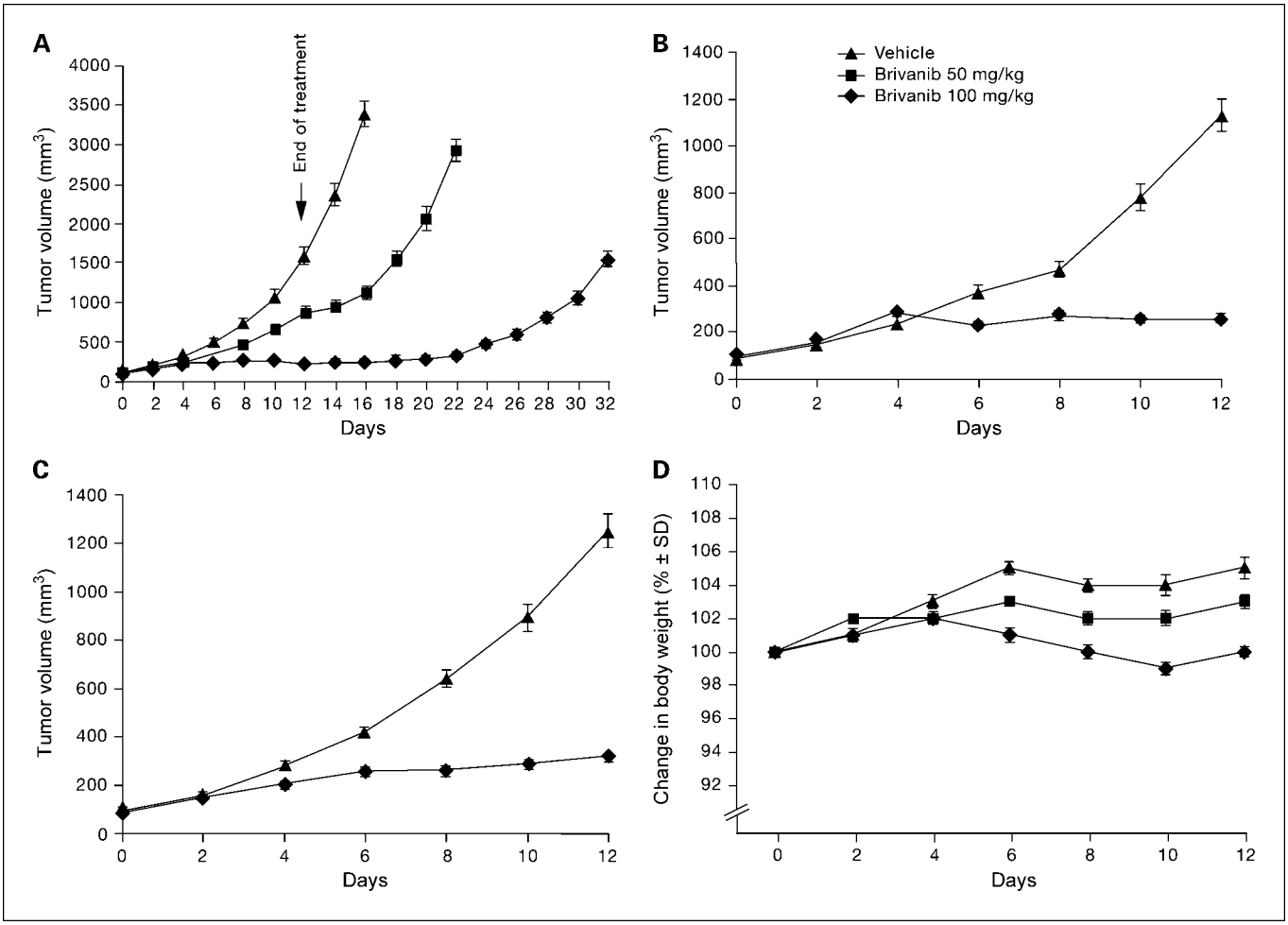

Fig. 2. Effects of brivanib on growth rate of patient-derived HCC xenograft lines 06-0606, 2-1318, and 26-1004. *A,* mice bearing xenograft line 06-0606 were treated with vehicle, 50 mg/kg brivanib, or 100 mg/kg brivanib daily for 12 d. *B* and *C,* mice bearing xenograft lines 2-1318 and 26-1004, respectively, were treated with 100 mg/kg brivanib daily for 12 d. Each treatment arm involved 14 independent tumor-bearing mice representing the same xenograft line. Points, mean tumor volume at given time points; bars, SE. Significant differences in tumor growth between vehicle-treated and brivanib-treated tumors were also observed as early as day 10 ($P < 0.01$). Note that brivanib had continued antitumor activity after cessation of treatment. *D,* percent change in body weight in mice treated with vehicle, 50 mg/kg brivanib and 100 mg/kg brivanib.

Table 1. Changes in body weight, tumor weight, microvessel density (CD31), markers of cell proliferation (Ki-67), and apoptosis (cleaved caspase-3) in mice treated with either vehicle or brivanib (100 mg/kg) in six HCC xenograft lines

Xenograft line	Treatment	Body weight at sacrifice (g)	Tumor weight at sacrifice (mg)	Microvessel density*	Ki-67 index (%)	Cleaved caspase-3 (%)
2-1318	Vehicle	23.4 ± 1.7	950 ± 1.9	27 ± 5	20 ± 4.6	5.1 ± 3
	Brivanib	22.5 ± 1.4	360 ± 49†	6 ± 3†	4.5 ± 2.7†	12.2 ± 3†
5-1318	Vehicle	22.6 ± 1.1	880 ± 121	29 ± 7	19.8 ± 4	3.6 ± 1.8
	Brivanib	22.2 ± 0.6	350 ± 69†	8.6 ± 4†	5.1 ± 1.8†	12.4 ± 2.4†
26-1004	Vehicle	23.9 ± 1.3	1080 ± 13	27 ± 7	19.8 ± 6.1	3.5 ± 1.7
	Brivanib	21.8 ± 0.7	371 ± 69†	5.8 ± 3†	7.5 ± 2.9†	11.8 ± 2.1†
30-1004	Vehicle	25.0 ± 1.3	798 ± 65	15.4 ± 4	16.2 ± 4	2.7 ± 1.2
	Brivanib	24.2 ± 1.0	480 ± 54†	7.3 ± 3†	8.5 ± 2.1†	8.8 ± 1.8†
2006	Vehicle	18.6 ± 0.9	650 ± 83	18.4 ± 5	13.2 ± 2.9	3.1 ± 1.4
	Brivanib	18.9 ± 0.6	250 ± 57†	5.2 ± 3†	4.8 ± 1.2†	12.3 ± 2.1†
06-0606	Vehicle	23.8 ± 0.8	1369 ± 24	30.8 ± 8	27.9 ± 5	1.2 ± 0.5
	Brivanib	23.5 ± 0.9	184 ± 43†	7 ± 3†	6.4 ± 3.1†	18.9 ± 2.3†

*Mean microvessel density of 10 random 0.159 mm^2 fields at ×100 magnification.
†$P < 0.001$ versus vehicle in same xenograft line.

endogenous peroxidase activity and nonspecific staining, the sections were incubated overnight at 4°C with the primary antibodies against CD31, Ki-67, and cleaved caspase-3 used to assess microvessel density, cell proliferation, and apoptosis, respectively.

Immunohistochemistry was done using the streptavidin-biotin peroxidase complex method according to the manufacturer's instructions (Lab Vision). For Ki-67, only the nuclear immunoreactivity was considered positive. The number of Ki-67–positive cells among at least 500 cells per region was counted and expressed as percentage values. For the quantification of mean microvessel density in sections stained for CD31, 10 random 0.159-mm^2 fields at ×100 magnification were captured for each tumor.

Statistical analysis. The differences in tumor growth among the treatment groups, body weight, tumor weight at sacrifice, mean microvessel density, percentage of Ki-67–positive cells, and cleaved caspase-3–positive cells were compared using ANOVA. Experiments were repeated at least thrice.

Results

As shown in Fig. 2A, the growth rate of tumors in mice with patient-derived xenograft line 06-0606 was decreased by brivanib treatment in a dose-dependent manner ($P < 0.01$). Tumor weights in these mice that were treated with 50 and 100 mg/kg brivanib by gavage daily for 12 days were approximately 55% and 13%, respectively, compared with vehicle-treated mice. Furthermore, brivanib, at a dose of 100 mg/kg, also inhibited tumor growth in mice with patient-derived xenograft lines 2-1318 (Fig. 2B) and 26-1004 ($P < 0.01$; Fig. 2C). Maximal inhibition was seen at 100 mg/kg in all patient-derived xenograft lines (Table 1). The T/C ratios for xenograft lines 2-1318, 5-1318, 26-1004, 30-1004, 2006, and 06-0606 were 0.38, 0.40, 0.34, 0.60, 0.38, and 0.13, respectively, after 12 days of treatment. Furthermore, growth suppression was seen in 06-0606, 2-1318, and 26-1004 xenograft lines 7 days after treatment (Fig. 2). As the 100 mg/kg daily dose gave maximal growth inhibition, this dose was used for all subsequent studies. Brivanib also inhibited the growth of the 26-1004 xenograft line in an orthotopic model (Supplementary Fig. S1). No overt toxicity, as defined by weight loss (Fig. 2D), unkempt appearance, mortality, and behavior, was observed in either brivanib treated or vehicle-treated mice during the course of treatment (data not shown).

No significant difference in VEGFR-2 levels was observed among six xenograft lines studied (Fig. 3). Variable levels of each FGFR were detected with the exception of the xenograft line 06-0606, which expressed all four FGFRs. Interestingly, this

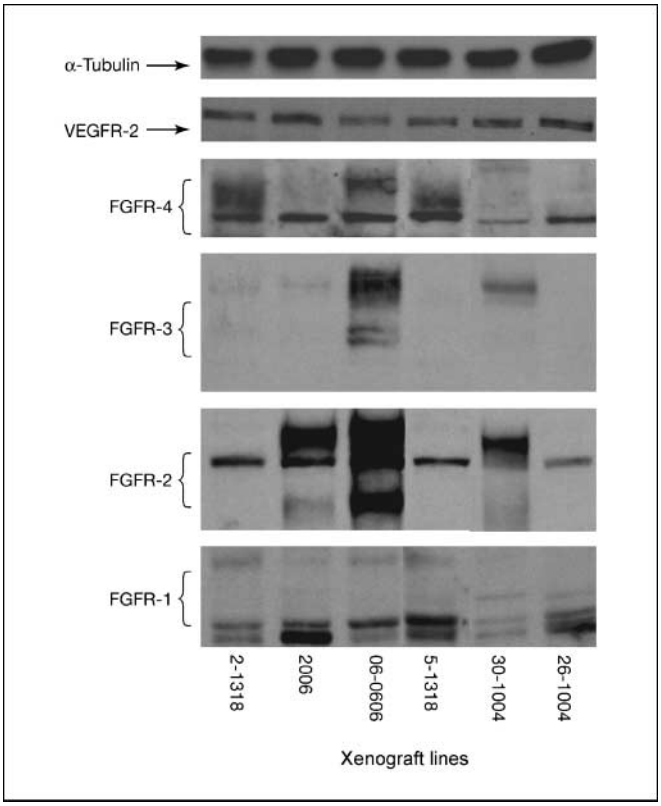

Fig. 3. Basal levels of FGFR-1, FGFR-2, FGFR-3, and FGFR-4 in patient-derived HCC xenografts. Expression of FGFR-1, FGFR-2, FGFR-3, and FGFR-4 on tumor xenograft lines is shown in a representative Western blot. Note that all xenograft lines react with some or all FGFRs, and expression varies in intensity and molecular size.

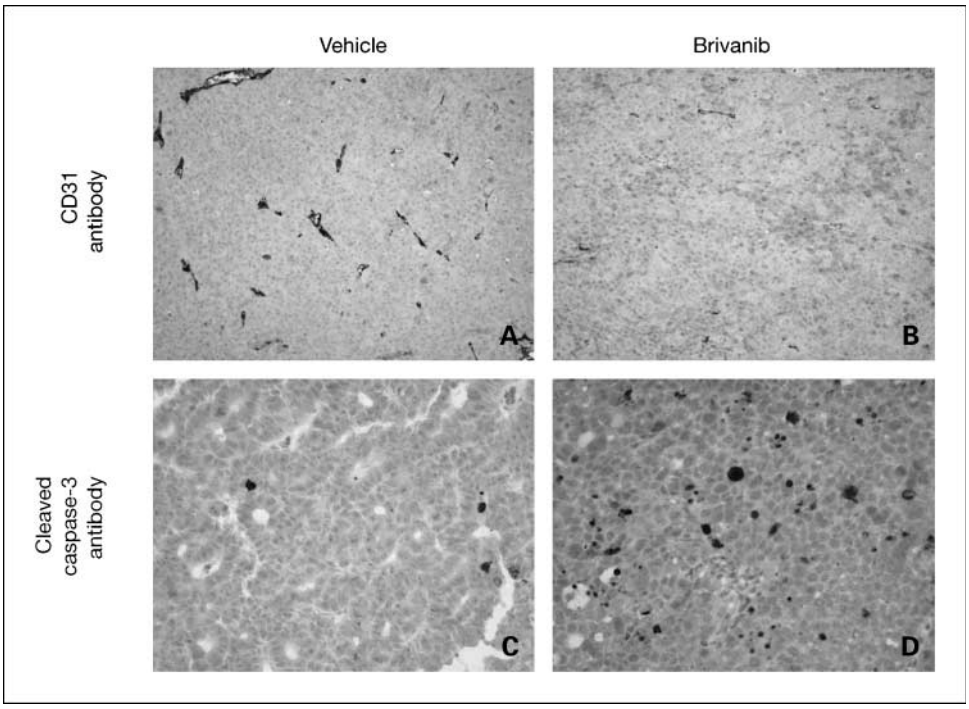

Fig. 4. Effects of brivanib therapy on neovascularization and apoptosis of xenograft line 06-0606. Representative pictures of the blood vessels stained with anti-CD31 (*A* and *B*) and cleaved caspase-3–positive cells (*C* and *D*) in vehicle-treated and brivanib-treated mice, respectively. Treatment with brivanibresulted in decreased vessel density and increased cell death.

line seemed to have the greatest sensitivity to brivanib as measured by the T/C ratio (Fig. 3).

The treatment with brivanib led to significantly decreased mean blood microvessel density, which is consistent with inhibition of angiogenesis, in all patient-derived xenografts tested with the greatest decrease in the xenograft line 06-0606 ($P < 0.01$; Fig. 4). Furthermore, the median number of CD31-positive endothelial cells in brivanib-treated mice was significantly reduced in all six patient-derived xenograft lines compared with control ($P < 0.01$; Table 1).

Immunohistochemical analysis revealed that the Ki-67 labeling index was significantly decreased in all six brivanib-treated xenograft lines compared with control ($P < 0.01$; Table 1). The percentage of cells stained for cleaved caspase-3 was significantly increased in brivanib-treated tumors ($P < 0.01$; Fig. 4; Table 1), suggesting that brivanib caused apoptosis of HCC cells. Again, the greatest changes in Ki-67 labeling and cleaved caspase-3 staining were in the xenograft line 06-0606.

The activation status of VEGFR-2 was investigated in xenograft lines 06-0606 and 26-1004 after 12 days of treatment with brivanib or control. Although there was no significant increase in VEGFR-2 expression, the levels of phosphorylated VEGFR-2 at $Tyr^{1054/1059}$, Akt at Ser^{473}, and ERK1/2 at Thr^{202}/Tyr^{204} in the brivanib-treated tumors were significantly decreased ($P < 0.01$), suggesting that the VEGFR-2 was inactivated (Fig. 5). No significant changes in FGFR-1 protein expression levels were observed in both xenograft lines 06-0606 and 26-1004 (Fig. 5). Brivanib induced significant reductions in the levels of Cdk-4, cyclin B1, and phospho-c-Myc ($P < 0.01$; Fig. 5). Moreover, brivanib also significantly increased the levels of cleaved caspase-3 and cleaved PARP without altering the levels of Bcl-x, Bcl-2, Bad, and Bax ($P < 0.01$; Fig. 5), indicating that brivanib may induce apoptosis by Bcl-2–independent mechanisms. There were no significant alterations in the levels of Cdk-6, E2F1, pRB, p130 RB, $p27^{Kip1}$, $p21^{WAF1}$, and cyclin A in brivanib-treated mice (data not shown).

To address the mechanism by which brivanib inhibits tumor growth, we evaluated the effect of brivanib on the phosphorylation levels of VEGFR-2 and FGFR-1, and their downstream signaling pathways, ERK1/2 and Akt, in SK-HEP1 cells and HepG-2 cells. In nonstimulated SK-HEP1 cells, brivanib alone had little effect on levels of phosphorylated ERK1/2, Akt, VEGFR-2, and FGFR-1. However, in VEGF- and bFGF-stimulated cells, brivanib significantly inhibited VEGFR-2, FGFR-1, ERK1/2, and Akt phosphorylation (Fig. 6A). In contrast, brivanib had no effects on IGF-1–induced ERK1/2 and Akt phosphorylation (Fig. 6B). Total VEGFR-2, FGFR-1, ERK1/2, and Akt levels were unchanged.

Discussion

This study showed that brivanib effectively inhibits tumor growth in five of six patient-derived human HCC xenograft lines. Furthermore, brivanib-induced growth inhibition was associated with inactivation of VEGFR-2, increased apoptosis, a reduction in microvessel density, inhibition of cell proliferation, and down-regulation of cell cycle regulators, including cyclin D1, Cdk-2, Cdk-4, cyclin B1, and phospho-c-Myc. Indeed, cell cycle arrest due to a reduction in positive cell cycle regulators may be responsible for the observed growth inhibition. It has previously been shown that conditional expression of the *c-Myc* oncogene in mouse liver results in the development of HCC (36). Treatment with brivanib also led to a decrease in the number of proliferating cells compared with control. The exact mechanisms by which brivanib treatment induces growth inhibition are not well understood. A previous study (13) has shown that brivanib affected the host endothelium based on both *in vitro* and *in vivo* studies (vascular density, Matrigel plugs, and dynamic

contrast-enhanced magnetic resonance imaging responses). It had no antiproliferative effects on L2987 lung carcinoma, HCT116 colon carcinoma, H3396 breast carcinoma, and CWR-22 prostate carcinoma cell lines in culture. Our present study shows that brivanib also acts *in vitro* on endothelial cells (Fig. 6A) and HepG2 cells (Fig. 6C) when stimulated with VEGF or FGF (Fig. 6A), suggesting that depending on the cell types studied brivanib may also have direct tumor activity *in vivo*. Brivanib may prevent the tumor mass from expanding by cutting off the supply of nutrients and growth factors to the tumor cells. In addition, the percentage of cells stained with cleaved caspase-3 was significantly increased in brivanib-treated tumors compared with control, suggesting that brivanib caused apoptosis of HCC cells.

It was shown that the six patient-derived HCC xenograft lines expressed all four FGFRs to varying levels; levels of FGFR-1 expression were lower in xenograft line 30-1004 compared with the other five xenograft lines, which correlates well with its sensitivity to brivanib. In addition, the xenograft line 06-0606, which expresses high levels of all four FGFRs, was particularly sensitive to brivanib, suggesting that the expression of FGFR-2, FGFR-3, and FGFR-4 may also contribute to its response toward brivanib. In this study, multiple forms of FGFR-2 were detected in xenograft lines 06-0606, 2006, and 30-1004. The exact role of FGFR-2 and its variants in HCC growth and angiogenesis remains to be elucidated. However, it should be noted that the xenograft line 06-0606 expressed very high levels of FGFR-2. It has been reported that somatic missense mutations of FGFR-2 are implicated in tumorigenesis, which has also been shown in cell lines of multiple tumor types and primary tumors (37, 38). Further studies are under way to investigate the role of FGFR-2 and its variants in angiogenesis and the development and progression of HCC. Additional evidence for the tumor growth-inhibitory effects of brivanib being due to its effects on VEGFR-2 and FGFR-1 was shown in SK-HEP1 cells, hepatocellular adenocarcinoma cells of endothelial origin.

Targeted inhibition of angiogenesis and induction of apoptosis using a dual inhibitor of VEGFR and FGFR tyrosine kinases may represent a good alternative treatment to currently available options for patients with HCC. Most patients present clinically with late-stage HCC with some individuals already

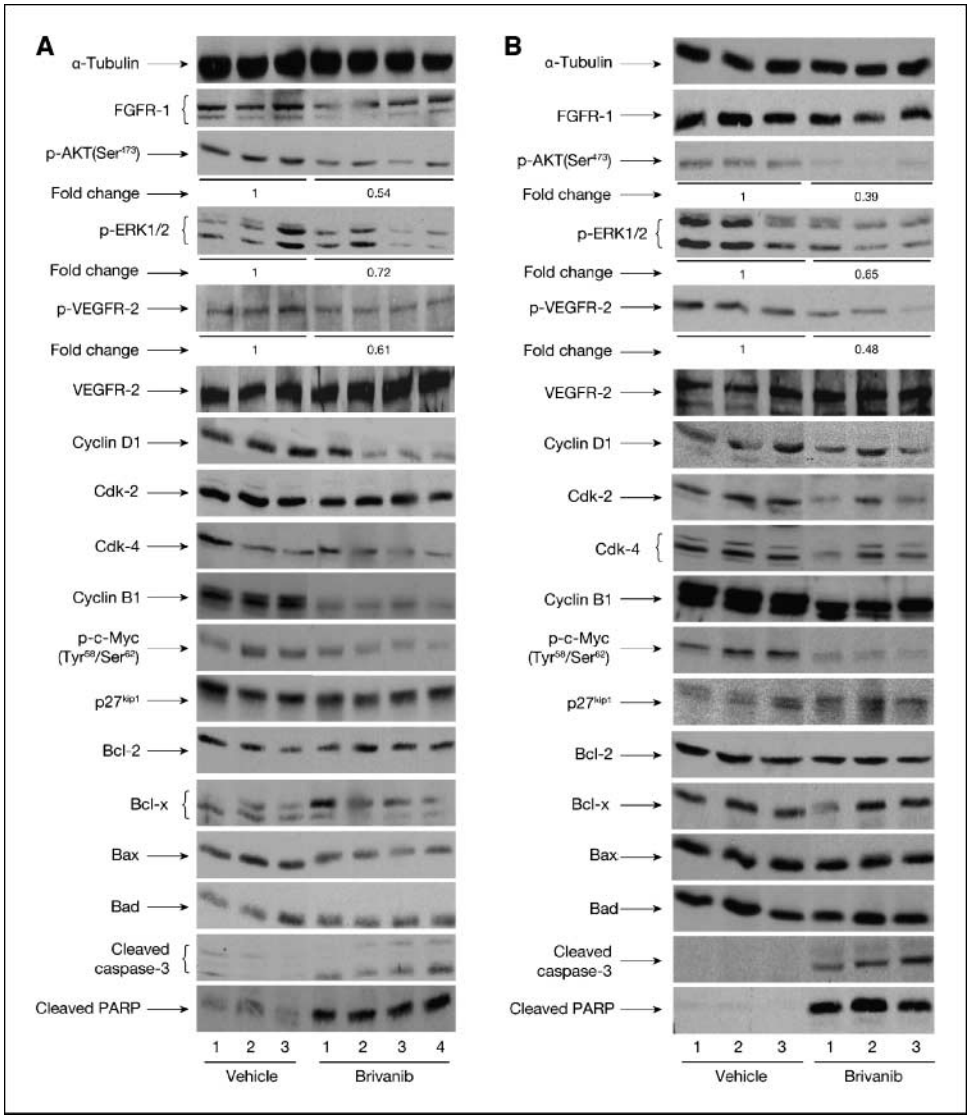

Fig. 5. Effects of brivanib on VEGFR-2 activity, cell proliferation, and apoptosis in HCC xenograft lines 06-0606 (*A*) and 26-1004 (*B*). Xenograft lines were stained with phospho-VEGFR-2, cell cycle markers, apoptotic regulators, cleaved caspase-3, and cleaved PARP. A representative Western blot shows a significant decrease in phospho-VEGFR-2, phospho-Akt, and phospho-ERK1/2; a significant decrease in cyclin D1, Cdk-2, Cdk-4, cyclin B1, and phospho-c-Myc; and a significant increase in cleaved caspase-3 and PARP ($P < 0.01$ for all conditions).

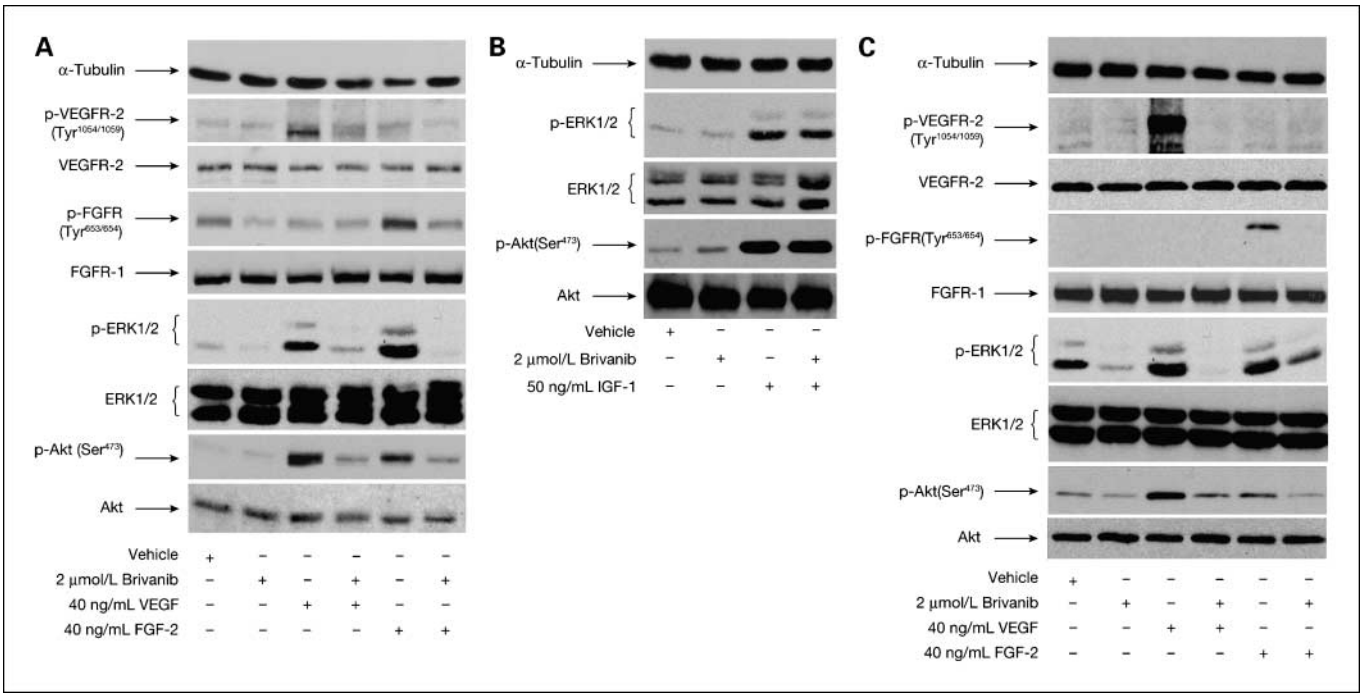

Fig. 6. Effects of brivanib on (*A* and *C*) VEGF-induced, bFGF-induced, and (*B*) IGF-I – induced phosphorylation of VEGFR-2, FGFR, Akt, and ERK1/2 in SK-HEP1 (*A* and *B*) and HepG2 (*C*) cells. Treatment of SK-HEP1 (*A*) and HepG2 (*C*) cells with brivanib significantly inhibited VEGFR-2, FGFR, ERK1/2, and Akt phosphorylation. IGF-I – induced ERK1/2 and Akt phosphorylation in SK-HEP1 cells was not affected by brivanib (*B*).

having widespread tumor dissemination. Patients who have undergone liver transplantation, resection, or liver-directed therapy have the greatest likelihood of developing primary or recurrent HCC. Therefore, the potent antiangiogenic activity of brivanib makes this drug potentially useful in maintaining dormancy of micrometastasis and preventing the development of recurrence or metastasis after surgical resection of a primary tumor. Furthermore, brivanib showed direct growth inhibition and induction of apoptosis. These effects may be mediated through FGF because FGFRs are present on endothelial cells and represent a critical signaling pathway for tumors. Although several new chemotherapies have been explored and refined in the last decade, the mortality rate due to HCC remains unchanged. New therapeutic strategies for HCC treatment are urgently needed. The important roles of the VEGF and FGF signaling pathways in promoting tumor angiogenesis and metastasis, together with its negative prognostic significance in HCC, make them appropriate therapeutic targets.

Disclosure of Potential Conflicts of Interest

Mark Ayers and Joseph Fargnoli are employees of Bristol-Myers Squibb.

References

1. Jemal A, Murray T, Ward E, et al. Cancer statistics, 2005. CA Cancer J Clin 2005;55:10–30.
2. Smith RA, Cokkinides V, Eyre HJ. American Cancer Society guidelines for the early detection of cancer, 2005. CA Cancer J Clin 2005;55:31–44.
3. Nagasue N, Kohno H, Chang YC, et al. Liver resection for hepatocellular carcinoma. Results of 229 consecutive patients during 11 years. Ann Surg 1993; 217:375–84.
4. Yamamoto J, Kosuge T, Takayama T, et al. Recurrence of hepatocellular carcinoma after surgery. Br J Surg 1996;83:1219–22.
5. Colombo M. Hepatocellular carcinoma. J Hepatol 1992;15:225–36.
6. Lai EC, Fan ST, Lo CM, et al. Hepatic resection for hepatocellular carcinoma. An audit of 343 patients. Ann Surg 1995;221:291–8.
7. Takenaka K, Kawahara N, Yamamoto K, et al. Results of 280 liver resections for hepatocellular carcinoma. Arch Surg 1996;131:71–6.
8. Zhu AX. Systemic therapy of advanced hepatocellular carcinoma: how hopeful should we be? Oncologist 2006;11:790–800.
9. Gish RG, Porta C, Lazar L, et al. Phase III randomized controlled trial comparing the survival of patients with unresectable hepatocellular carcinoma treated with nolatrexed or doxorubicin. J Clin Oncol 2007;25: 3069–75.
10. Yeo W, Mok TS, Zee B, et al. A randomized phase III study of doxorubicin versus cisplatin/interferon α-2b/ doxorubicin/fluorouracil (PIAF) combination chemotherapy for unresectable hepatocellular carcinoma. J Natl Cancer Inst 2005;97:1532–8.
11. Abou-Alfa GK, Schwartz L, Ricci S, et al. Phase II study of sorafenib in patients with advanced hepatocellular carcinoma. J Clin Oncol 2006;24:4293–300.
12. Llovet J, Ricci S, Mazzaferro V, et al for the SHARP Investigators Study Group. Sorafenib in advanced hepatocellular carcinoma (HCC). Lancet 2008;359: 378–90.
13. Bhide R, Cai Z-W, Zhang Y-Z, et al. Discovery and preclinical studies of (*R*)-1-(4-(4-fluoro-2-methyl-1*H*-indol-5-yloxy)-5-methylpyrrolo[2,1-*f*][1,2,4]triazin-6-yloxy)propan- 2-ol (BMS-540215), an *in vivo* active potent VEGFR-2 inhibitor. J Med Chem 2006; 49:2143–6.
14. Mise M, Arii S, Higashituji H, et al. Clinical significance of vascular endothelial growth factor and basic fibroblast growth factor gene expression in liver tumor. Hepatology 1996;23:455–64.
15. Kim KW, Bae SK, Lee OH, Bae MH, Lee MJ, Park BC. Insulin-like growth factor II induced by hypoxia may contribute to angiogenesis of human hepatocellular carcinoma. Cancer Res 1998;58:348–51.
16. Park BC, Huh MH, Seo JH. Differential expression of transforming growth factor α and insulin-like growth factor II in chronic active hepatitis B, cirrhosis and hepatocellular carcinoma. J Hepatol 1995;22:286–94.
17. Seo JH, Kim KW, Murakami S, Park BC. Lack of colocalization of HBxAg and insulin like growth factor II in the livers of patients with chronic hepatitis B, cirrhosis and hepatocellular carcinoma. J Korean Med Sci 1997;12:523–31.
18. Miura H, Miyazaki T, Kuroda M, et al. Increased expression of vascular endothelial growth factor in human hepatocellular carcinoma. J Hepatol 1997;27: 854–86.
19. Torimura T, Sata M, Ueno T, et al. Increased expression of vascular endothelial growth factor is associat-

ed with tumor progression in hepatocellular carcinoma. Hum Pathol 1998;29:986–91.

20. Poon RT, Ng IO, Lau C, et al. Correlation of serum basic fibroblast growth factor levels with clinicopathological features and postoperative recurrence in hepatocellular carcinoma. Am J Surg 2001;182:298–304.

21. Jinno K, Tanimizu M, Hyodo I, et al. Circulating vascular endothelial growth factor (VEGF) is a possible tumor marker for metastasis in human hepatocellular carcinoma. J Gastroenterol 1998;33:376–82.

22. Li X, Tang Z, Zhou G. Expression if vascular endothelial growth factor correlates with invasion and metastasis of hepatocellular carcinoma. Zhonghua Zhong Liu Za Zhi 1998;20:12–4.

23. Moon WS, Rhyu KH, Kang MJ, et al. Overexpression of VEGF and angiopoietin 2: a key to high vascularity of hepatocellular carcinoma? Mod Pathol 2003;16:552–7.

24. Poon RT, Ng IO, Lau C, et al. Serum vascular endothelial growth factor predicts venous invasion in hepatocellular carcinoma: a prospective study. Ann Surg 2001;233:227–35.

25. Poon RT, Lau C, Yu WC, Fan ST, Wong J. High serum levels of vascular endothelial growth factor predict poor response to transarterial chemoembolization in hepatocellular carcinoma: a prospective study. Oncol Rep 2004;11:1077–84.

26. Moscatelli D, Joseph-Silverstein J, Presta M, Rifkin DB. Multiple forms of an angiogenesis factor: basic fibroblast growth factor. Biochimie 1988;70:83–7.

27. Hsu PI, Chow NH, Lai KH, et al. Implications of serum basic fibroblast growth factor levels in chronic liver diseases and hepatocellular carcinoma. Anticancer Res 1997;17:2803–9.

28. Ingber D. Extracellular matrix and cell shape: potential control points for inhibition of angiogenesis. J Cell Biochem 1991;47:236–41.

29. El Assal ON, Yamanoi A, Ono T, Kohno H, Nagasue N. The clinicopathological significance of heparanase and basic fibroblast growth factor expressions in hepatocellular carcinoma. Clin Cancer Res 2001;7:1299–305.

30. Poon RT, Ng IO, Lau C, Yu WC, Fan ST, Wong J. Correlation of serum basic fibroblast growth factor levels with clinicopathologic features and postoperative recurrence in hepatocellular carcinoma. Am J Surg 2001;182:298–4.

31. Yoshiji H, Kuriyama S, Yoshii J, et al. Synergistic effect of basic fibroblast growth factor and vascular endothelial growth factor in murine hepatocellular carcinoma. Hepatology 2002;35:834–42.

32. Kin M, Sata M, Ueno T, et al. Basic fibroblast growth factor regulates proliferation and motility of human hepatoma cells by an autocrine mechanism. J Hepatol 1997;27:677–87.

33. Huynh H, Soo KC, Chow PK, Panasci L, Tran E. Xenografts of human hepatocellular carcinoma: a useful model for testing drugs. Clin Cancer Res 2006;12:4306–14.

34. Heffelfinger SC, Hawkins HH, Barrish J, Taylor L, Darlington GJ. SK HEP-1: a human cell line of endothelial origin. In Vitro Cell Dev Biol 1992;28A:136–42.

35. Huynh H, Chow PK, Ooi LL, Soo KC. A possible role for insulin-like growth factor-binding protein-3 autocrine/paracrine loops in controlling hepatocellular carcinoma cell proliferation. Cell Growth Differ 2002;13:115–22.

36. Shachaf CM, Kopelman AM, Arvanitis C, et al. MYC inactivation uncovers pluripotent differentiation and tumor dormancy in hepatocellular cancer. Nature 2004;431:1112–7.

37. Jang JH, Shin KH, Park JG. Mutations in fibroblast growth factor receptor 2 and fibroblast growth factor receptor 3 genes associated with human gastric and colorectal cancers. Cancer Res 2001;61:3541–3.

38. Greenman C, Stephens P, Smith R, et al. Patterns of somatic mutation in human cancer genomes. Nature 2007;446:153–8.